Journal of Solid State Chemistry **157,** 86–93 (2001)
doi:10.1006/jssc.2000.9042, available online at http://www.idealibrary.com on IDEAL®

Epitaxial Growth of Ag_2S Film on Cleaved Surface of MgO(001)

Hiroshi Nozaki,[1] Mitsuko Onoda, Keiji Kurashima, and Takahumi Yao*

*National Institute for Research in Inorganic Materials, 1-1 Namiki, Tsukuba, Ibaraki 305-0044, Japan; and *Institute for Materials Research, Tohoku University, 2-1-1 Katahira, Aoba-ku, Sendai 980-0000, Japan*

Received August 3, 2000; in revised form November 1, 2000; accepted December 1, 2000

Epitaxial films of monoclinic Ag_2S with various thicknesses were prepared on cleaved surfaces of MgO(001) by molecular beam epitaxy. The epitaxial relations of the films to the substrates were determined by X-ray diffractometry. For thin films, there are three kinds of crystallites with (012), (−112), and (040) parallel to $(001)_{MgO}$. These are all equivalent in the high-temperature cubic form of Ag_2S, corresponding to {110}. With respect to epitaxy within the substrate surface for the crystallites, the diagonal direction of the body-centered pseudocubic sulfur arrays of Ag_2S, [100] and [201], are parallel to $[100]_{MgO}$, which is due to the coincidence of lattice dimensions of the film and substrate. For thick films, the epitaxial relations are $(-112)//(001)_{MgO}$ and $[421]//[010]_{MgO}$, or $(012)//(001)_{MgO}$ and $[4, -2, 1]//[010]_{MgO}$. The epitaxy for thick films is restricted not only by the surface periodicity of the substrate but also by the existence of steps generated during cleaving. The textures of thick films observed by polarized microscopy confirm that the epitaxial growth of the thick films is restricted by the steps.

Key Words: **epitaxial growth; epitaxy; silver sulfide; magnesium oxide; substrate; cleaved surface.**

INTRODUCTION

Heteroepitaxial growth of β-Ag_2S (argentite, stable between 177 and 593°C (1)), a superionic conductor, is of interest because it is expected that mobile silver atoms could adjust their arrangement among the interstices of the sulfur lattice to absorb strain, owing to the lattice periodicity of the substrate surface, that is, epitaxial growth of the compound could be relatively easily realized (2). The structure of β-Ag_2S is cubic, space group $Im3m$, with a body-centered cubic array for the sulfur ions. The lattice constant at 186°C is 0.4860 nm (1). Upon cooling below 177°C, it transforms itself into the α-phase (acanthite, monoclinic, space group $P21/c$), which is stable at room temperature. The lattice constant of α-Ag_2S is $A = 0.4231$ nm, $B = 0.6930$ nm, $C = 0.9526$ nm, and $\beta = 125.48°$ (3). The monoclinic cell contains two pseudocubic subcells with an average lattice dimension of 0.485 nm. The $\beta \rightarrow \alpha$ transition upon cooling inevitably causes an aggregate of polysynthetically twinned crystals of the low temperature form on α-Ag_2S film. Thus, of further interest is the manner in which the texture of α-Ag_2S film is affected by the surface condition of the substrate employed.

An epitaxial thin film of Ag_2S has been prepared on a cleaved NaCl(001) substrate (4). The epitaxial orientation varies with increasing film thickness from pseudocubic triclinic (110) orientation in the initial stage to monoclinic (012) orientation in the final stage (nominal film thickness 2.4 nm) via a monoclinic (010) orientation, where the (110) orientation denotes $(110)_{film}//(001)_{NaCl}$. It has been pointed out that the transformation process of the film structure is expressed by a change in position of the smaller mobile silver ions in the rigid lattice of sulfur ions (2). The epitaxial relationships of Ag_2S to AgBr(001) and AgBr(111) substrates have also been reported (5). The preparation of Ag_2S films deposited on glass substrates has been intensively studied with emphasis on semiconductive properties (6, 7).

In the present investigation, the heteroepitaxial growth of Ag_2S on a cleaved MgO(001) substrate, which depends on film thickness, is reported. Ag_2S films were prepared in a range of thickness wider than that of the films in the previous studies mentioned above. The texture of the Ag_2S film is also dependent on the film thickness. We thought that ionic crystals like MgO as well as NaCl and AgBr, which were easily cleaved, were adequate as a substrate for the epitaxial growth of Ag_2S, because our preliminary experiment showed no epitaxial growth for a Ag_2S film prepared on Si(001) with typically covalent bonding character.

EXPERIMENTAL

Deposition experiments were carried out by molecular beam epitaxy (MBE; EpiQuest Co., type miniMBee). The molecular beam of silver was made by controlling the temperature of a pyrolytic boron nitride (p-BN) crucible cell

[1]To whom correspondence should be addressed. E-mail: nozaki@nirim.go.jp.

0022-4596/01 $35.00

containing silver (purity, 99.999%). The temperature of the crucible, which was thermally shielded by four cylindrical tantalum sheets, was measured by a WRe5-26 thermocouple kept in contact with the bottom of the crucible. The beam intensity was calibrated by a naked ionization gauge before and after each deposition experiment. The sulfur molecular beam intensity was also controlled by varying the temperatures at three places, i.e., at a stainless steel bath used as a sulfur (purity 6N) source, at the conducting pipe with a needle valve, and at the cracking cell. It was also controlled by manually adjusting the opening ratio of the needle valve. The temperature of the cracking cell was always set at 500°C. The sulfur molecular beam intensity was also measured by the naked ionization gauge before and after the experiment. The p-BN crucible and cracking cells were isolated by a liquid N_2 shroud. Experiments were carried out at background pressures below 6×10^{-7} Torr when the needle valve controlling sulfur pressure was opened and below 1×10^{-9} Torr when it was closed. MgO(001) substrates used (15×15 mm^2 in area and 0.5 to ~ 1 mm in thickness) were cleaved in a clean room, attached mechanically to a molybdenum disk, and set in the vacuum system after about 15 min. The molybdenum disk with the substrate was fixed to a manipulator by a pair of arc-shaped molybdenum arms. A WRe5-26 thermocouple was welded to one of the arms for monitoring the substrate temperature. The substrates were kept at about 700°C for 30 min under gaseous pressures below 1×10^{-9} Torr by heating the opposite side of the molybdenum disk. The substrate temperatures were then kept between 270 and 300°C for the present deposition experiments. The substrate temperature was monitored by a radiation thermometer and the above thermocouple, which were calibrated by measuring the melting point of Sn film (about 10 nm) deposited on MgO(001). The surface state of the substrate was examined by reflection high energy electron diffractometry (RHEED) before the deposition experiment.

Ag_2S films of various thicknesses were prepared; 9.8, 48.9, and 84.9 nm with a silver deposition rate of 0.045 nms^{-1} and 339 nm with a rate of 0.20 nms^{-1}. Their thicknesses are nominal, estimated from the products of silver deposition rate and deposition time. The film with nominal thickness of 9.8 nm in Ag deposition is denoted as Film 9.8 for simplicity and the other films are similarly denoted Films 48.9, 84.9, and 339. These films were deposited under a stoichiometric sulfur excess, because the sticking coefficient for sulfur on silver was estimated to be 0.25 (8). After the deposition experiments, the Ag_2S films were slowly cooled (0.8°C/min near the α/β transition temperature) to room temperature.

The epitaxial characteristics of the Ag_2S films were examined by an X-ray powder diffractometer equipped with a line-focused Cu$K\alpha$ source and a curved incident monochromater of pyrolytic graphite (002). Reflections for the lattice planes of Ag_2S film parallel to the substrate surface $(001)_{MgO}$ were easily collected in ordinary θ–2θ scanning mode. Reflections for those inclined to $(001)_{MgO}$ were measured by setting offset angles for the θ axis corresponding to the facial angles between the lattice planes epitaxially parallel to $(001)_{MgO}$ and the lattice planes in question, as estimated from the lattice parameters of Ag_2S.

The textures of the epitaxial Ag_2S films were examined by polarized microscopy using transmitted polarized light.

EXPERIMENTAL RESULTS

X-ray reflections for Ag_2S lattice planes parallel to $(001)_{MgO}$ for Film 339 were collected by ordinary diffractometry, as shown in Fig. 1: -112 and 012 and their multiples were observed. The reflections marked by an asterisk in the figure result from the MgO substrate, which includes reflections due to $\lambda/2$ and $\lambda/3$ as well as λ, the wavelength of Cu$K\alpha$. It is noted that the intensity of -112 is about three times larger than that of 012. The intensity ratio between -112 and 012 depends on film thickness, as shown in Fig. 2a, where the reflection profile for Film 9.8 is assumed to resolve into components of 020, -112, and 012 reflections. It is noted in Figure 2a that (1) the relative intensity of 012 to that of -112 increases with decreasing film thickness, (2) half-value widths of the -112 and 012 components for film 9.8 are several times larger than those of the other films, and (3) the 020 reflection is observed only for film 9.8. The thickness dependence of 040, -224, and 024 reflection profiles is shown in Fig. 2b. It is also noted in the figure that the same tendencies are observed with respect to the relative intensities of -224 and 024 and with respect to the half-value widths of these reflections as observed in the -112 and 012 reflections. We note also that the relative intensity of 040 to -224 and 024 increases with decreasing film thickness.

In addition to these reflections for the lattice planes parallel to $(001)_{MgO}$, reflections for lattice planes inclined to

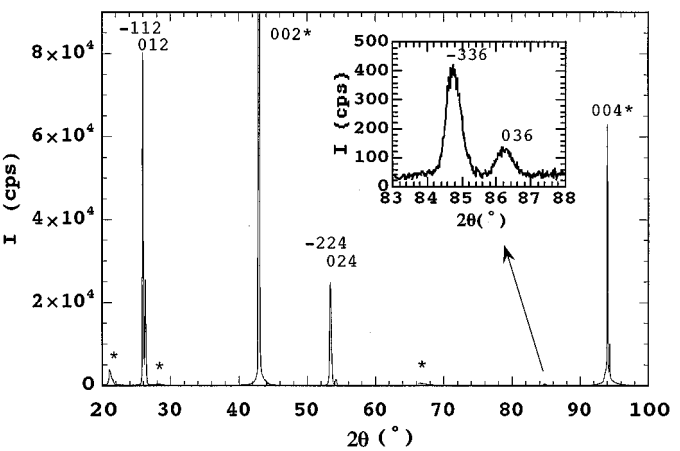

FIG. 1. X-ray diffraction pattern for Film 339 taken in the ordinary θ–2θ scan mode.

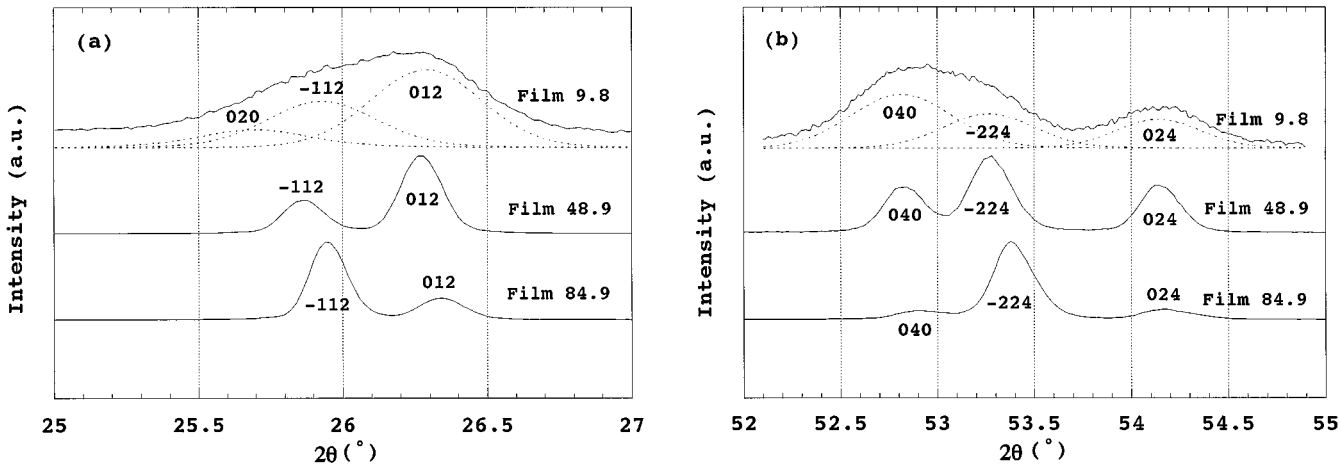

FIG. 2. Thickness dependence of reflection profiles: (a) 020, −112, and 012 reflections and (b) 040, −224, and 024 reflections.

$(001)_{MgO}$ were collected. The half-value widths of the reflection profiles were in the range 0.14° and 0.35° for Films 339, 84.9, and 48.9 and between 0.45° and 0.61° for Film 9.8. The reflections observed for lattice planes parallel and inclined to $(001)_{MgO}$ are summarized in Tables 1–4, where the reflections were collected by setting $[100]_{MgO}$ parallel to the direction of the θ axis, except 132 for Film 48.9. In the tables, facial angles observed and calculated between (012) and lattice planes inclined to (012), (0kl), and (132) are listed; the facial angles of (− 232), (− 344), and (− h, h, 2h) to (− 112) together with the facial angles of (0, 2k, 0) to (040) are also listed. The observed angles were used to determine the indices of the reflections in question. The lattice parameters for Films 339, 84.9, and 48.9 are also shown in Tables 1–3, respectively. Those for Film 9.8, however, were not obtained but B and $C \sin \beta$ were calculated by the least-squares method, because d spacings apart from those of indices 0kl and −112 and their multiples could not be collected. The thickness dependence of B and $C \sin \beta$ is shown in Fig. 3. The magnitude of B decreases with increasing thickness but that of $C \sin \beta$ increases with thickness. It should be noted that the magnitude of B estimated from the d spacing of 040 ($\times$ in the figure), which is the d spacing for the crystallite with (040) parallel to $(001)_{MgO}$, is systematically lower than that estimated from the d values of 0kl indices by the least-squares method for crystallites with (012) parallel to $(001)_{MgO}$.

The textures of Films 339 and 84.9 were clearly observed to be aggregates of very large crystallites (about 100 μm), as shown in Fig. 4a, by a transmitted polarized light. A photograph for Film 339 was quite similar to that for Film 84.9. Portions with the same contrast in Fig. 4a indicate crystallites with the same orientation. The microscope pattern of the texture varied with rotating the film around the ray axis of polarized light. It is found that crystallites for Films 339 and 84.9 grow along steps on the cleavage surface of

TABLE 1
X-Ray Diffraction Data for Film 339

h	k	l	d_{obs}	d_{cal}	ϕ_{obs}	ϕ_{cal}	I_{obs}
−1	1	2	3.4362	3.4358	0.00	0.00	100
0	1	2	3.3832	3.3914	0.00	0.00	30
0	1	3	2.4249	2.4296	8.85	8.81	1
0	2	3	2.0818	2.0746	7.40	7.52	<1
0	1	4	1.8808	1.8737	13.6	13.7	<1
−2	2	4	1.7173	1.7179	0.00	0.00	30
0	2	4	1.6907	1.6957	0.00	0.00	2
−2	3	2	1.5527	1.5493	26.1	27.2	<1
1	3	2	1.5371	1.5370	26.6	26.6	1
−3	3	6	1.1455	1.1453	0.00	0.00	<1
−3	4	4	1.0937	1.0940	19.0	18.8	<1

Note. $A = 0.4244$ nm; $B = 0.6904$ nm; $C = 0.9530$ nm; $\beta = 125.67°$.

TABLE 2
X-Ray Diffraction Data for Film 84.9

h	k	l	d_{obs}	d_{cal}	ϕ_{obs}	ϕ_{cal}	I_{obs}
−1	1	2	3.4355	3.4356	0.00	0.00	100
0	1	2	3.3839	3.3855	0.00	0.00	16
0	1	3	2.4261	2.4233	8.61	8.77	<1
0	2	3	2.0747	2.0728	7.31	7.50	<1
0	4	0	1.7286	1.7328	0.00	0.00	1
−2	2	4	1.7158	1.7178	0.00	0.00	11
0	2	4	1.6903	1.6927	0.00	0.00	1
−2	3	2	1.5412	1.5445	26.1	27.1	1
0	1	5	1.5131	1.5144	16.4	16.6	<1
−1	1	6	1.5029	1.5064	25.7	26.0	<1
0	6	0	1.1533	1.1552	0.00	0.00	<1
−3	3	6	1.1439	1.1452	0.00	0.00	<1
−3	4	4	1.0915	1.0915	18.7	18.8	<1

Note. $A = 0.4216$ nm; $B = 0.6931$ nm; $C = 0.9552$ nm; $\beta = 125.67°$.

TABLE 3
X-Ray Diffraction Data for Film 48.9

h	k	l	d_{obs}	d_{cal}	ϕ_{obs}	ϕ_{cal}	I_{obs}
−1	1	2	3.4398	3.4398	0.00	0.00	100
0	1	2	3.3880	3.3853	0.00	0.00	98
0	1	3	2.4226	2.4228	8.69	8.77	14
0	2	3	2.0727	2.0731	7.40	7.49	5
0	1	4	1.8707	1.8676	13.5	13.6	3
0	4	0	1.7316	1.7345	0.00	0.00	9
−2	2	4	1.7186	1.7199	0.00	0.00	9
0	2	4	1.6930	1.6927	0.00	0.00	6
1	3	2	1.5400	1.5400	26.4	26.6	<1
0	1	5	1.5136	1.5140	16.6	16.6	1
0	3	4	1.4856	1.4859	10.8	10.8	<1
0	6	0	1.1544	1.1563	0.00	0.00	1
0	3	6	1.1283	1.1284	0.00	0.00	1

Note. $A = 0.4254$ nm; $B = 0.6938$ nm; $C = 0.9491$ nm; $\beta = 125.19°$.

$(001)_{MgO}$ and also extend from step to step, as shown in Fig. 4a, where steps are seen as stripes. Another texture pattern appeared after rotation of about $\pm 35°$ from the angle at which the photograph of texture (Fig. 4a) was taken. By contrast, the sizes of crystallites for Films 48.9 and 9.8 must be very small (less than 1 μm), because textures such as those observed for Films 339 and 84.9 were not found, as shown in Fig. 4b. A photograph for Film 48.9 was quite similar to that for Film 9.8.

DISCUSSION

Epitaxy of Thin Film

There are three kinds of Ag_2S crystallites with lattice planes parallel to $(001)_{MgO}$: (-112), (012), and (040). These planes for the monoclinic lattice of the low temperature form correspond to $(011)_c$, $(101)_c$, and $(220)_c$ for the cubic lattice of the high temperature form, where monoclinic and cubic lattice planes are hereafter denoted as $(hkl)_m$ and $(hkl)_c$, respectively. These monoclinic or cubic lattice planes are most dense in the sulfur packing of the body-centered lattice. The relations between the monoclinic lattice vectors (shown in capital letters) and the cubic ones (in small letters) are $\boldsymbol{A} = (\boldsymbol{a} - \boldsymbol{b} - \boldsymbol{c})/2$, $\boldsymbol{B} = \boldsymbol{a} + \boldsymbol{b}$, and $\boldsymbol{C} = 2\boldsymbol{c}$.

Many $0kl$ reflections were observed for Films 9.8 and 48.9, when [100] of MgO was set parallel to the θ axis of the goniometer. It is noted that the intensities of the $0kl$s for Films 9.8 and 48.9 are relatively strong in comparison with those for Films 339 and 84.9. The $(0kl)_m$ planes are planes of a zone with zone axis $[100]_m$; that is, the epitaxial orientation within the substrate surface is $\boldsymbol{A}//[100]_{MgO}$ for crystallites with $(012)_m//(001)_{MgO}$.

The reflection 132 observed for Film 48.9 was collected by setting $[1, -\frac{1}{2}, \frac{1}{4}]_m$ parallel to the θ axis assuming that the angle between $[1, -\frac{1}{2}, \frac{1}{4}]_m$ and $\boldsymbol{A}$ is about 54.7° within $(012)_m$. The zone axis for $(132)_m$ and $(012)_m$ is $[1, -\frac{1}{2}, \frac{1}{4}]_m$. The observation of 132 for Film 48.9 is another confirmation of the epitaxial orientation $\boldsymbol{A}//[100]_{MgO}$.

It should be noted that the length of $\boldsymbol{A}$ (0.4254 nm) well agrees with the lattice parameter of MgO (0.4213 nm) and the periodicity perpendicular to $\boldsymbol{A}$ within $(012)_m$ is 0.40 nm, which almost agrees with the lattice parameter of the substrate. An Ag_2S island film on $(001)_{NaCl}$ in the previous study (thickness = 2.4 nm) has shown the same (012) orientation but different in-plane epitaxy relations probably due to the different lattice sizes of NaCl and MgO (4).

The vector $\boldsymbol{A}$ is parallel to the diagonal axis of the body-centered lattice with half the diagonal length. The similar diagonal vector, $\boldsymbol{G} = [1, 0, \frac{1}{2}]_m = (-\boldsymbol{a} + \boldsymbol{b} - \boldsymbol{c})/2$, equivalent to $\boldsymbol{A}$ in the cubic high temperature form, is the zone axis for $(-1, k, 2)_m$s. It would thus similarly be expected that, for a crystallite with $(-112)_m//(001)_{MgO}$, reflections for the lattice planes of $(-1, k, 2)_m$s might be observed. However, the substrate interrupts X-rays reflected by $(-1, k, 2)_m$s, because the facial angle of $(-1, k, 2)_m$ to $(-112)_m$ is larger than the Bragg angle θ_B except for $k = 1$.

The epitaxial orientation for the crystallites with $(-112)_m//(001)_{MgO}$ is probably $\boldsymbol{G}//[100]_{MgO}$, because the epitaxy relation of crystallites with $(-112)_m//(001)_{MgO}$ to the substrate surface must be equivalent to that of crystallites with $(012)_m//(001)_{MgO}$, when the substrate temperature is above the $\beta \rightarrow \alpha$ transition temperature and, further, because the subcell of the monoclinic structure below the transition temperature is pseudocubic.

Assuming $\boldsymbol{G}//[100]_{MgO}$ for the crystallites with $(-112)_m//(001)_{MgO}$, the length of $\boldsymbol{G}$ (0.423 nm) agrees well with the lattice parameter of MgO and the periodicity perpendicular to $\boldsymbol{G}$ within (−112) is 0.40 nm, which almost agrees with the lattice parameter of the substrate.

For the crystallites with $(040)_m//(001)_{MgO}$, reflections such as 031, 041, 042, and 043, might be expected to be observed, because the planes, $(040)_m$, $(031)_m$, $(041)_m$, $(042)_m$, and $(043)_m$, are planes of zone parallel to $\boldsymbol{A}$ and have facial

TABLE 4
X-Ray Diffraction Data for Film 9.8

h	k	l	d_{obs}	d_{cal}	ϕ_{obs}	ϕ_{cal}	I_{obs}
0	2	0	3.4634	–	0.00	–	24
−1	1	2	3.4332	–	0.00	–	60
0	1	2	3.3870	–	0.00	–	100
0	1	3	2.4215	–	8.81	–	25
0	2	3	2.0724	–	7.54	–	6
0	4	0	1.7317	–	0.00	–	15
−2	2	4	1.7181	–	0.00	–	9
0	2	4	1.6926	–	0.00	–	8

Note. $B = 0.6942$ nm; $C \sin \beta = 0.7754$ nm.

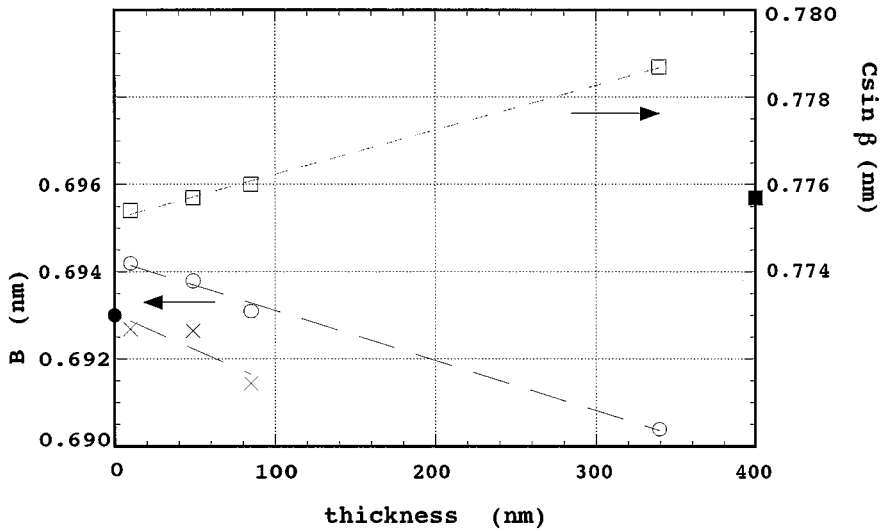

FIG. 3. Thickness dependence of B and $C \sin \beta$. The magnitude of B based on the d spacing of 040 is marked with an $\times$. The magnitudes of B and $C \sin \beta$ estimated from the lattice parameters previously reported are denoted by a solid circle and a solid square, respectively. "Thickness" in the abscissa is nominal thickness defined by amount of silver deposition.

angles smaller than their Bragg angles. However, the 031 reflection could not be observed, although the intensity of the reflection was estimated to be strong. This suggests that the number of crystallites with $(040)_m//(001)_{MgO}$ is much smaller than that of crystallites with $(012)_m//(001)_{MgO}$ after the cubic to monoclinic transition.

The plane $(040)_m$ includes $\boldsymbol{A}$; so $\boldsymbol{A}$ for the crystallites with $(040)_m//(001)_{MgO}$ is considered to be parallel to $[100]_{MgO}$ for the same reason as that of the case of crystallites with $(-112)_m//(001)_{MgO}$. That is, the periodicity perpendicular to A within $(040)_m$ is 0.39 nm, which is somewhat shorter than 0.40 nm for the crystallites with $(012)_m//(001)_{MgO}$ and also 0.40 nm for those with $(-112)_m//(001)_{MgO}$. This may cause the number of crystallites with $(040)_m//(001)_{MgO}$ to decrease.

Epitaxy of Thick Film

The lattice planes of $(-112)_m$ and $(012)_m$ for Film 339 are parallel to $(001)_{MgO}$, as seen in the diffraction pattern in Fig. 1. Among the reflections shown in Table 1, -232, -344, 132, and -116 were collected by setting offset angles around the θ axis. The planes $(-112)_m$, $(-232)_m$, and $(-344)_m$, which correspond to $(011)_c$, $(031)_c$, and $(042)_c$, respectively, are planes of zone with zone axis $[1, \frac{1}{2}, \frac{1}{4}]_m$, which corresponds to $[100]_c$. On the other hand, the lattice

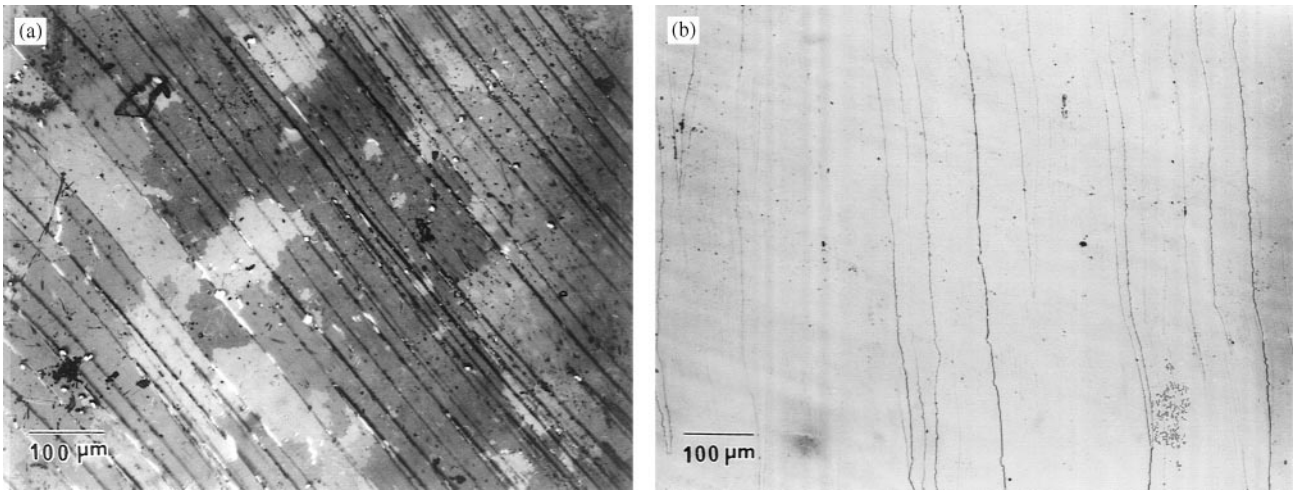

FIG. 4. Photographs of Ag_2S films taken by transmitted polarized microscopy. (a) Film 84.9 and (b) Film 9.8.

planes of $(012)_m$ and $(132)_m$, which correspond to $(101)_c$ and $(301)_c$, respectively, are planes of zone with zone axis $[-1, \frac{1}{2}, -\frac{1}{4}]_m$, which corresponds to $[010]_c$. Thus, the epitaxy relations of specimen Film 339 are

$[421]_m//[010]_{MgO}$ for crystallites with $(-112)_m//(001)_{MgO}$

and

$[4, -2, 1]_m//[010]_{MgO}$ for crystallites with $(012)_m//(001)_{MgO}$.

The epitaxy relation for Film 84.9 is the same as that for Film 339 except that the -116 reflection in place of 132 is used to determine the epitaxy relation, where $(-116)_m$ corresponds to $(103)_c$. The epitaxial relations for thin and thick Ag_2S films on $(001)_{MgO}$ are illustrated in Figs. 5a and 5b, respectively.

$0kl$ reflections with very weak intensities are also found for Film 339 and 84.9, as shown in Tables 1 and 2, which indicate that epitaxy similar to that observed for the thin film weakly coexists. The thickness dependence of relative intensity, I_{0kl}/I_{-112}, is plotted in Fig. 6. It is found here that the thickness dependence of relative intensity drastically changes below and above 84.9 nm. This clearly indicates the difference of epitaxy between thin and thick films.

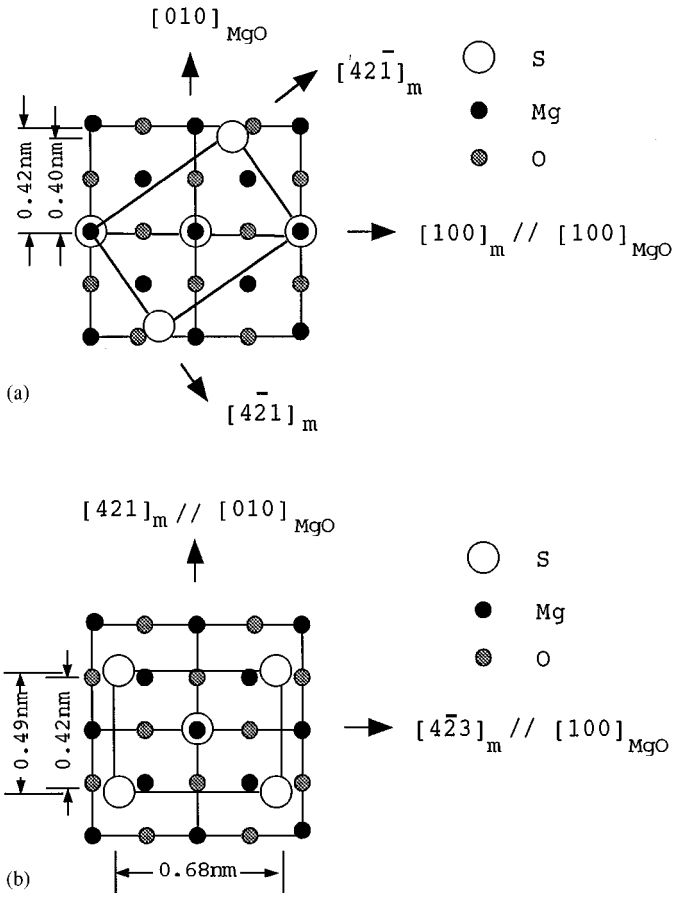

FIG. 5. Schematic illustration of epitaxy within the substrate surface. (a) $(012)_m$ orientation on MgO(001) for thin films and (b) $(-112)_m$ orientation for thick films. $(012)_m$ orientation denotes $(012)_m//(001)_{MgO}$.

Relation of Epitaxy to Substrate

The experimental results indicate that lattice planes dense in sulfur, i.e., $\{110\}_c$, are parallel to $(001)_{MgO}$ for both thin and thick films. The epitaxy within the substrate surface for the thin film is considered to be restricted by the coincidence between the lattice periodicities of film and substrate, as already mentioned and as shown in Fig. 5a. The lattice length of the thin film along ***A*** is 0.4% larger than the lattice constant of the substrate, and the length of the film along the direction perpendicular to ***A*** is 5.8% smaller than the lattice constant of the substrate for the crystallites with $(012)_m//[001]_{MgO}$.

On the other hand, the epitaxy within the substrate surface for the thick film is restricted not only by the lattice periodicity of the substrate surface but also by another factor, i.e., the existence of steps that are generated upon cleaving and have various heights of less than a few micrometers, with the exception of epitaxy for small areas of the film which is the epitaxy for the thin film. This is confirmed by the texture of the thick film (Fig. 4a), where crystal growth appears to start from steps and run over some flat surfaces extending from step to step. The step controls the direction of crystal growth, resulting in large crystallites (about 100 μm). This indicates that the epitaxy is also restricted by the existence of steps, as well as the surface lattice of $(001)_{MgO}$. The epitaxy for the thick film (Fig. 5b) is consistent with the above statement. Texture like that for the thick films, Nos. 339 and 84.9, was not observed for the thin films, Nos. 48.9 and 9.8, under polarized microscope. This is probably due to the small size of the crystallites in the thin films, where the existence of steps may not significantly affect the crystal growth of the films.

For the crystallites with $(-112)_m//(001)_{MgO}$, the lattice length of the thick film along $[4, -2, 3]_m$, 0.677 nm, is 60% larger than the lattice constant of the substrate, and the lattice length of the film along $[4, 2, 1]_m$, 0.489 nm, is also 16% larger than the lattice constant of the substrate, as shown in Fig. 5b. This means that there exist 5×6 lattice units of Ag_2S within the area of 8×7 lattice units of MgO. For the crystallites with $(012)_m//[001]_{MgO}$, the lattice length along $[4, 2, -1]_m$ and that along the direction perpendicular to this are 0.688 and 0.489 nm, respectively. For the crystallites with $(040)_m//[001]_{MgO}$, which were slightly observed for Film 84.9 and not observed for Film 339, the lattice length along $[4, 0, 1]_m$ and that along the perpendicular direction (***C***) are 0.689 and 0.476 nm, respectively. For both latter crystallites, coincidence between the lattice lengths of Ag_2S and MgO seems to be more wrong than that for the crystallite with $(-112)_m//(001)_{MgO}$. This may be the

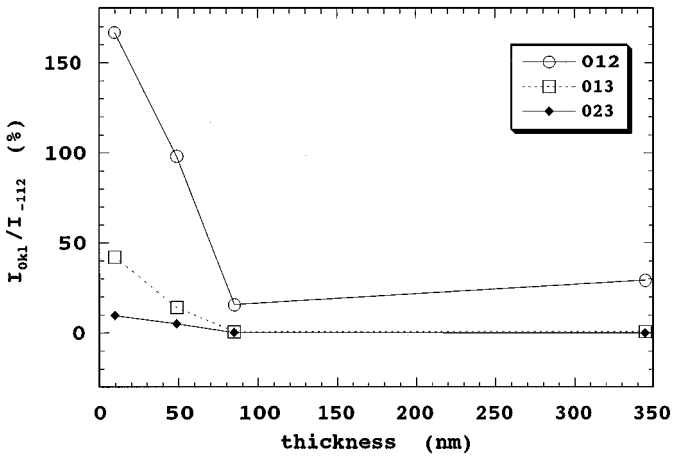

FIG. 6. Thickness dependence of relative intensity. The ordinate is the ratio of intensity for $0kl$ to that for -112. The abscissa is nominal thickness defined by amount of silver deposition.

reason that for thick films the $(-112)_m$ orientation is more preferential than the $(012)_m$ orientation and further the $(040)_m$ orientation was slightly observed only for Film 84.9.

The parameter $\boldsymbol{B}$ decreases with increasing film thickness, while the parameter C sin β increases, as shown in Fig. 3. It should be noted that these parameters are those for the crystallites with $(012)_m//(001)_{MgO}$ and $\boldsymbol{A}//[100]_{MgO}$. The magnitudes of $\boldsymbol{B}$ and C sin β for Film 84.9 almost agree with the magnitudes obtained from the reported lattice parameters of Ag_2S (3), 0.693 and 0.776 nm, respectively.

The angle between $\boldsymbol{B}$ and $(012)_m$ is about 30° and the projection of $\boldsymbol{B}$ onto $(012)_m$ is perpendicular to $\boldsymbol{A}$. The lattice length of substrate along $[010]_{MgO}$ makes the lattice dimension of Ag_2S elongated along this direction, which results in elongation of $\boldsymbol{B}$ for the thin films, Nos. 9.8 and 48.9. On the other hand, the elongation of $\boldsymbol{B}$ makes C sin β decrease, assuming that the length of $\boldsymbol{A}$ is almost fixed because of the good agreement between the length of $\boldsymbol{A}$ and the lattice dimension of the substrate and assuming that the cell volume does not change.

The magnitude of C sin β for the thick film, No. 339, is larger than the magnitude 0.776 nm mentioned above and that of B is smaller than the magnitude 0.693 nm. It is considered from the X-ray reflection intensity for Film 339 (Table 1) that the number of crystallites with $(012)_m//(001)_{MgO}$ and $\boldsymbol{A}//[100]_{MgO}$ is significantly smaller than that with $(-112)_m//(001)_{MgO}$ and $[421]_m//[010]_{MgO}$. The magnitude C Sin β is equal to the interplane spacing of $(001)_m$ and the facial angle between $(001)_m$ and $(012)_m$ is about 29°. Further, the d spacing of $(-112)_m$ is larger by 1.5% than that of $(012)_m$.

It is thus naturally inferred that the d spacing of $(012)_m$ elongates if a crystallite with $(012)_m//(001)_{MgO}$ and $\boldsymbol{A}//[100]_{MgO}$ is adjacent to a crystallite with $(-112)_m//(001)_{MgO}$ and $[4, 2, 1]_m//[010]_{MgO}$. This may result in the increase of C Sin β over the magnitude 0.776 nm and the decrease of B below 0.693 nm. The alternative explanation for the larger C Sin β of No. 339 is due to twinning of crystallites. For an example, a crystallite with $(012)_m//(001)_{MgO}$ and $A//[100]_{MgO}$ can twin with a crystallite with $(-1, -1, 2)_m//(001)_{MgO}$ and $\boldsymbol{A} + \boldsymbol{C}/2//[100]_{MgO}$. The twinning plane for this case is $(010)_m$. The d spacing of $(-1, -1, 2)_m$ is larger by 1.5% than that of $(012)_m$. It may thus elongate C Sin β, if the strain resulting from the twinning plane is stronger than that from the substrate surface with increasing film thickness.

The magnitude B for the crystallites with $(012)_m//(001)_{MgO}$ and $\boldsymbol{A}//[100]_{MgO}$ is somewhat larger than the magnitude estimated from the d spacing of $(040)_m$, which belongs to the crystallites with $(040)_m//(001)_{MgO}$. This may suggest that there are differences between the lattice parameters of crystallites with different epitaxial orientations.

Finally, we discuss appearance of the reflection 020 for Film 9.8. The 040 reflection is mainly due to the periodicity of the silver layer perpendicular to $\boldsymbol{B}$, while the 020 reflection reflects the periodicity of the sulfur layer perpendicular to $\boldsymbol{B}$. Thus, the intensity of 040 is evidently stronger than that of 020 because of the difference of scattering factors for silver and sulfur, which explains why we did not observe 020 for Films 339, 84.9, and 48.9. The appearance of the 020 reflection for Film 9.8 suggests that the periodicity of the silver layer along B for a thin film such as No. 9.8 is modified by strain due to the lattice periodicity of the substrate surface.

The half-value widths of reflection profiles for Film 9.8 are larger than those for the other films and are proportional to tan θ, as shown in Fig. 7, although the data collection range of θ is rather narrow. This also suggests that the lattice parameters for Film 9.8 may fluctuate, probably

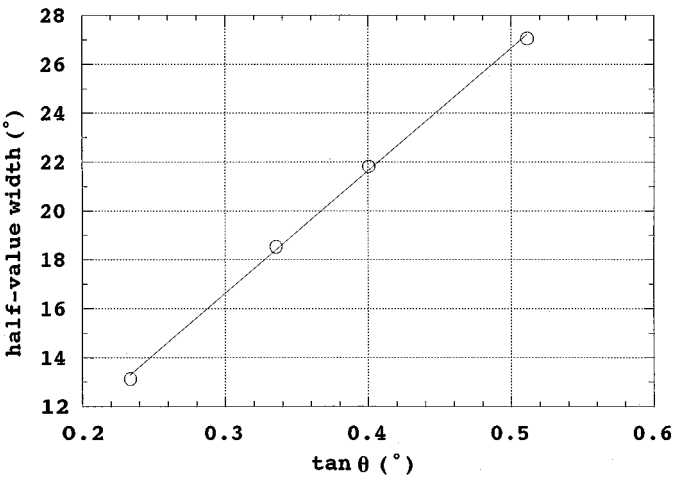

FIG. 7. Dependence of the half-value reflection width for Film 9.8 on tan θ (θ, Bragg angle).

dependent on the distance from the substrate surface. The larger half-value width for Film 9.8 and the appearance of the 020 reflection may be associated with the modified periodicity of silver layers along the *B* axis, as pointed out in the previous structure models of Ag_2S thin film on $(001)_{NaCl}$ (2).

ACKNOWLEDGMENTS

The authors thank Drs. H. Wada and M. Ishii (NIRIM) for their encouragements of this work. They thank Dr. J. R. Hester (Australian Beam line, KEK) for his critical reading of the manuscript and F. P. Okamura for his advice on the manuscript.

REFERENCES

1. R. J. Cava, F. Reidinger, and B. J. Wuensch, *J. Solid State Chem.* **31,** 69 (1980).
2. K. Bozhilov, V. Dimov, A. Panov, and H. Haefke, *Thin Solid Films* **190,** 129 (1990).
3. R. Sadanaga and S. Sueno, *Mineral. J.* **5,** 124 (1967).
4. H. Haefke, A. Panov, and V. Dimov, *Thin Solid Films* **188,** 133 (1990).
5. H. Haefke, H. Hofgmeister, M. Krohn, and A. Panov, *J. Imaging Sci.* **35,** 164 (1991).
6. B. R. Sankapal, R. S. Mane, and C. D. Lokhande, *Mater. Chem. Phys.* **63,** 226 (2000).
7. M. Amlouk, N. Brunet, B. Cros, S. Belgacem, and D. Barjon, *J. Phys. III* **7,** 1741 (1997).
8. T. Fleisch and R. Abermann, *Thin Solid Films* **42,** 255 (1977).